Landmine Detection by Correlation Method in Different Environments

A. Gharamohammadi[1,*], Y. Norouzi[2]

[1] Department of Electrical Engineering, Amirkabir University of Technology, Tehran, Iran
[2] Department of Electrical Engineering, Assistance prof. of Electrical Eng, Amirkabir University of Technology, Tehran, Iran

ARTICLE INFO	ABSTRACT
	In this paper, the purpose is the detection of a landmine in an environment using the scattering parameter. The Ground Penetrating Radar (GPR) measures the scattering parameter. The scattering parameter is taken from a simple environment in which a landmine exists alone as a reference signal. Signals taken from the complex environment are compared with the reference signal. In fact, the presence of a landmine influences the scattering parameter. The similarity between measured signal and reference signal determines the presence of the landmine. The correlation function calculates similarity. This method is very applicable because the scattering parameter is unique.

1. INTRODUCTION

One of the widely used tools to detect objects in a wide variety of applications, including landmine detection [1], Buried Pipe Detection [1], and Detecting oil under snow [3] is GPR. GPR is capable of detecting metallic and nonmetallic objects because it is sensitive to changes in electric permittivity, electric conductivity, and magnetic permeability. GPR has limitations, e.g its signal is attenuated by metallic objects and also, conductive and wet ground makes detection hard for GPR [4]. In Antarctica, GPR was used for ice sounding for the first time [5].

GPR usually operates in the frequency ranging from 1-5000 MHz [4]. Two traditional GPR systems exist, according to the radiated signal. Pulse radar systems that use small pulses of a short period (generally 1-10 nanoseconds) are commonly used. Other GPR systems use sinusoidal radio waves of a tone signal. This type of GPR is named Continuous Wave GPR (CW-GPR) [6].

A distinguished feature of Step Frequency Ground Penetrating Radar (SFGPR) is penetrating depth without lowering power [7]. Stepped-Frequency Continuous-Wave (SFCW) GPR is another system, suitable for detecting the buried pipelines. This type of GPR uses narrow IF bandwidth and high power, hence it has lower noise [5].

---

* Corresponding Author: A. Gharamohammadi
Department of Electrical Engineering, Amirkabir University of Technology, Tehran, Iran

The landmine detection is essential for mankind but also expensive because of its unclear position [8,9]. Several methods are utilized to detect landmines including video impulse GPR system [8], multiple landmine detection[1], the Acoustic laser method [10], clutter modelling [11], Prony's algorithm[12], Complex-valued neural networks[13], Bispectrum method[14] and Karhunen-Loeve (KL) transform[15,16].

In the video impulse GPR system, an FR-127-MSCB impulse GPR is used for measurements and a fuzzy logic-based algorithm uses the similarity of prototypes or feature sets for landmine detection [8].

The algorithm of multiple landmine detection uses symmetry filtering for extracting signals for each object and energy projection for estimating the number of objects. In this method, the envelope detector is used in landmine detection [1].

Parametric acoustic array (PAA) source in Acoustic laser method is used to transmit a sound beam from a safe distance. The standoff system concept is used and discussed in this method [10].

The clutters have an essential role in detection of small objects in the heterogeneous soil. Hence, GPR clutter has influenced the propagation of electromagnetic waves [11].

Prony's algorithm finds the domain complex natural resonances (CNRs) for vectors of the time-domain. In this method, the distance-based detectors process an unknown image with CNR features known objects [12].

The neural network can be used for landmine detection. The data is provided by different kinds of sensors. The classification on phase-sensitive detection has provided detection of the landmine by a complex-valued neural network [13]. In another method, Bispectrum is used to extract shape-dependent features. A neural network is trained on the feature extracted from the image window. The trained network performs detection and classification. For example, KL transform is used to extract features [14-16].

Scattering parameter (s-parameter) was used to detect the buried objects and small cracks and holes in metals and other materials [2,17]. Modelling the environment using a lumped element model is an approximate model [2]. The scattering parameter depends on some parameters of the object such as size, shape, composition, and permittivity. Hence, we can get some properties of the object from it [18]. S-parameter is used to detect a tumor in the brain and lungs. In this method, s-parameter is transformed to the time domain by Inverse Fast Fourier Transform (IFFT) and the process is applied on the time-domain signal. This method uses the peak of time-domain signal when the tumor is present and absent with each other for detection of the tumor [19-21].

In this paper, two kinds of simulations are done. In the first kind landmine is present and in another it is absent. Hence, a method for deciding on the presence of a landmine is selected. We choose the correlation method between two signals. All plots in the simulation part demonstrate the ability of this method. In this method, there is a restriction on the substance of the soil layer. If the wet soil was close to the surface of the ground, good results could not be obtained. GPR can-not obtain good results when the wet soil in the environment exists as in figure 8 and results are shown in figure 9. However, in our environment, the soil is dry so this method can help us very well.

2. SCATTERING PARAMETER

The scattering parameter can be calculated according to the incident and reflected waves. The incident wave illuminates the target and is produced by a transmitter antenna. The reflected wave is scattered from target and received by receiving antenna [2]. Scattering regions are regions that are classified according to the wavelength and size of the target. The Rayleigh scattering region is located where the size of the object is smaller than the wavelength. The object size in the resonant scattering region is more than 10λ [22]. In this paper, the landmine is on the resonant scattering region. Standing wave and travelling wave are measured mixtures together in one direction in one-point. They can be calculated rarely independent and they are dependent on the frequency. Hence, impedance or admittance are not good displays, for this reason, we use the scattering parameter [23]. For the N-port network, the scattering matrix(s-matrix) is defined as the impedance or admittance matrix. S-matrix is calculated according to the incident wave and reflected wave. The environment can be modelled like a circuit and calculated s-matrix. is the amplitude of incident voltage wave and is the amplitude of reflected voltage wave[24]. The S-matrix relates these two parameters to each other. The following formula shows it.

$$
\begin{pmatrix} V_1^- \\ V_2^- \\ . \\ . \\ . \\ V_N^- \end{pmatrix} = \begin{pmatrix} S_{11} & S_{12} & . & . & . & S_{1N} \\ S_{21} & S_{22} & . & . & . & S_{2N} \\ . & . & . & . & . & . \\ . & . & . & . & . & . \\ . & . & . & . & . & . \\ S_{N1} & S_{N2} & . & . & . & S_{NN} \end{pmatrix} \begin{pmatrix} V_1^+ \\ V_2^+ \\ . \\ . \\ . \\ V_N^+ \end{pmatrix}
\tag{1}
$$

Or

$$
\left(V^- \right) = (S)(V^+)
\tag{2}
$$

Where $S_{i\,j}$ is defined as

$$
S_{ij} = \frac{V_i^-}{V_j^+} \bigg|_{V_k^+ = 0 \ \ for \ k=1,2,...,j-1,j+1,...,N}
\tag{3}
$$

Here, S_{ij} means transmission coefficient from port j to port i when other ports are terminated in the matched load. We can calculate S_{12} by applying an incident wave to the port 2 and calculate the output wave from port 1 [24].

The S-matrix of the reciprocal network is symmetrical by calculating the S-parameter. It is defined as

$$
(s) = (s)^t
\tag{4}
$$

Where t means the transpose matrix.
Likewise for a lossless network, the following expression can be obtained

$$
\sum_{k=1}^{N} S_{k\,i} \, S_{k\,i}^* = 1
\tag{5}
$$

Where * means the conjugate matrix.

$$
\sum_{k=1}^{N} S_{k\,i} \, S_{k\,j}^* = 0, \ for \ i \neq j
\tag{6}
$$

3. CORRELATION FUNCTION

The correlation function is defined as

$$
R_{vw}(q) \triangleq \int_{-\infty}^{+\infty} v(s) w^*(s-q) ds
\tag{7}
$$

In this method, the scattering signal is complex. Hence, the correlation is also a complex number. In this paper, similarity is demonstrated based on magnitude. For this reason, normalization is used.

$$P_v \triangleq \left\langle \ v(t)v(t)^* \right\rangle \geq 0 \tag{8}$$

P for two signals that are similar is the power of the signal [25].

4. SIMULATION ANALYSIS

The GPR is appropriate to detect objects with a size of 5-30 centimeters (cm) [26]. The S-parameter can be used for the detection of a plastic landmine by using the simulation of a simple and complex real environment in Computer System Technology software (CST).

In this paper, the landmine is made from polyimide. It is loaded from the material library of CST. Its epsilon is 3.5 and mue is 1. The radius of the landmine is 5 cm and the height is 15 cm. Sandy soil epsilon is 2.53 and mue is 1. The distance between the landmine peak and soil surface is 5 cm. Figure 1 shows an a landmine alone in dry soil.
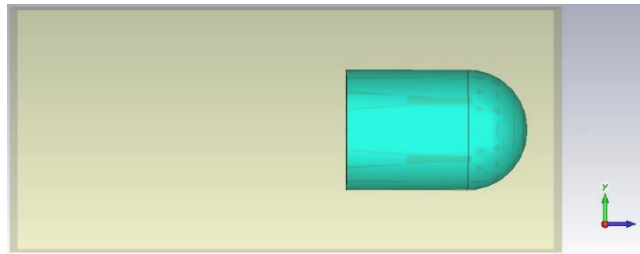

Fig. 1. Landmine alone in simple environment

A GPR is simulated with two inputs and two outputs. For these purposes, two Vivaldi antenna are dedicated that can radiate and receive wave. The location of antennas in all simulations is constant. The transmitted signal plot in figure 2. Figure 3 shows an antenna and Figure 4 shows antennas in the environment.

The environment boundary conditions are specified as a Perfectly Matched Layer (PML), meaning that lateral reflections have been eliminated. The distance between ports and surface of the soil is 1 cm. The first simulation is a landmine alone in dry soil that is shown in figure 1. The S-parameter matrix has been taken according to the frequency ranging from 600-2000 MHz. The s-parameter of this simulation is taken as a reference signal. Some simulations are shown in figures 5, 6, 7 and 8. İn figure 5, a brick concrete is put under a landmine and in figure 6, a pipe is put. Figure 7 shows a very complex environment. In figure 8, a 5 cm layer of moist soil is put in the surface. İn the other simulations, the landmine is absent. The similarity between simulations are calculated in table 1.
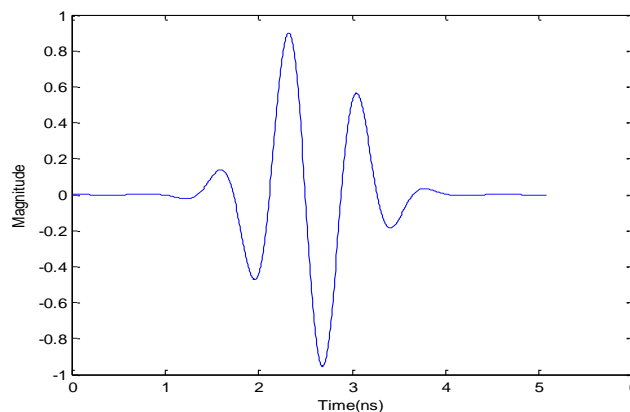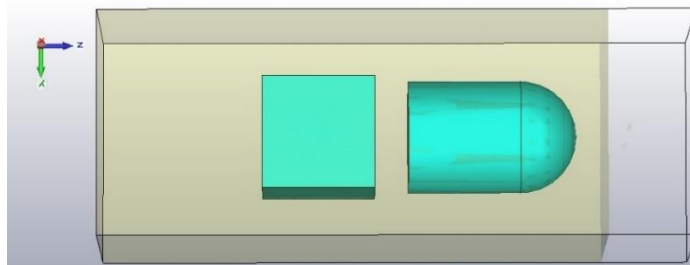

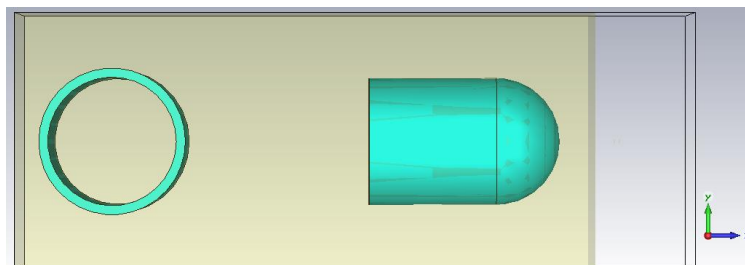**Fig. 2.** Transmitted signal in simulations
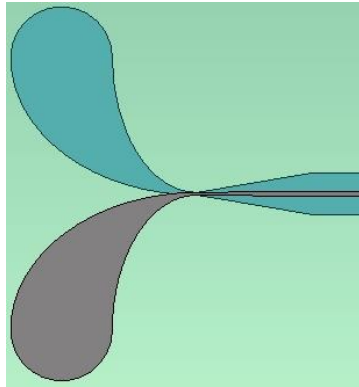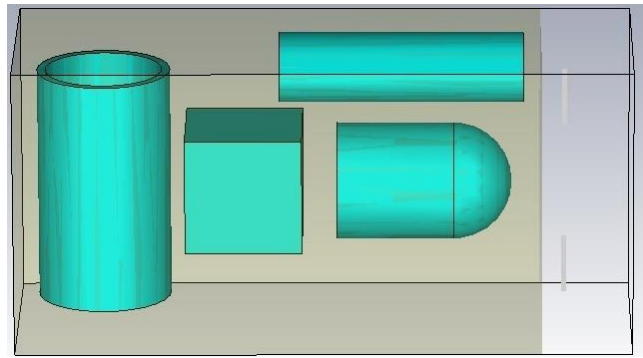
Fig. 3. Antenna
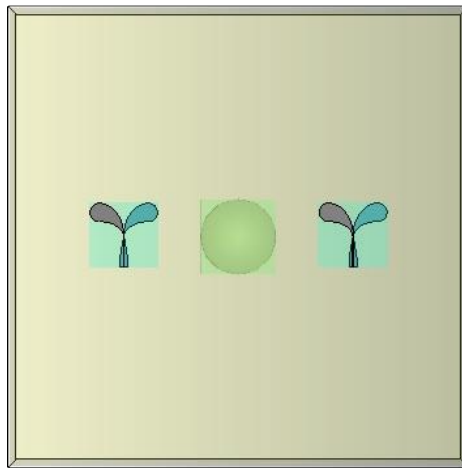
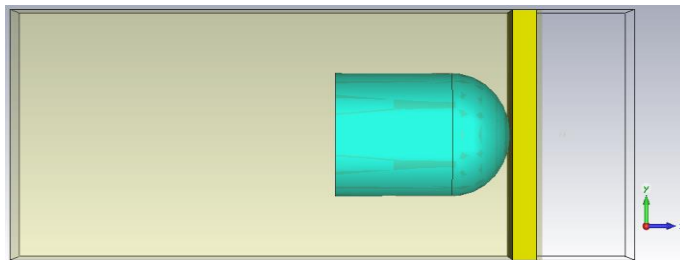**Fig. 4.** Antennas and environment with landmine from the top

Fig. 5. Environment simulated with a concrete brick under the landmine

Fig. 6. Environment simulated with a pipe under the landmine

Fig. 7. Complex environment simulated with a landmine

Fig. 8. Environment simulated with the landmine and a layer of moist soil in the surface

Table 1. Similarity

Type	Similarity(percentage)
figure 1a without landmine	50.2
Figure 3a	98.68
Figure 3a without landmine	54.29
Figure 4	99.26
Figure 4 without landmine	70.1
Figure 5a	99.11
Figure 6a	65.3

Figure 9 demonstrates s21 magnitude when the landmine is present or absent when a layer of wet soil is on the surface, compared with the reference signal.

For the wet soil, the other methods like time delay differences [27] and resistively Loaded Vee Dipoles can be used [28]. We cannot separate the effect of every object because the S-parameter behaves nonlinearly [24].

Figure 10 demonstrates that s21 magnitude is taken from figure 1, figure 7 and figure 7 when the landmine is absent in one plot.

In figure 11, the impact of each of the objects is shown. The black line shows S21 from dry soil. It is obvious that the red line is different from the others. The green and blue lines are very similar to the black line. It is very clear that the soil effect is undeniable.
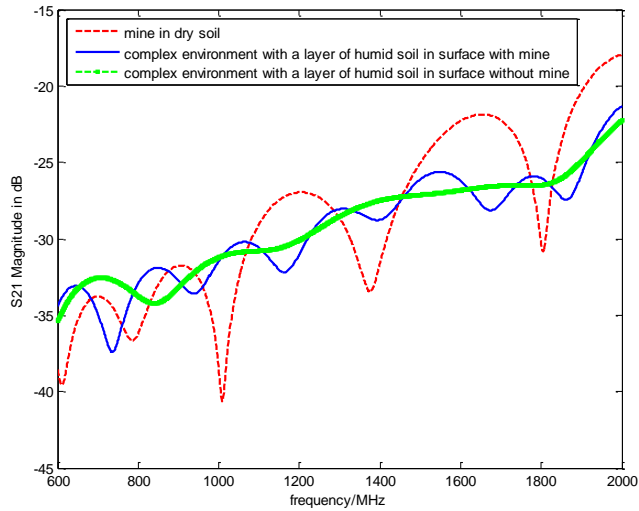
Fig. 9. Received signals for understanding the effect of a layer of moist soil
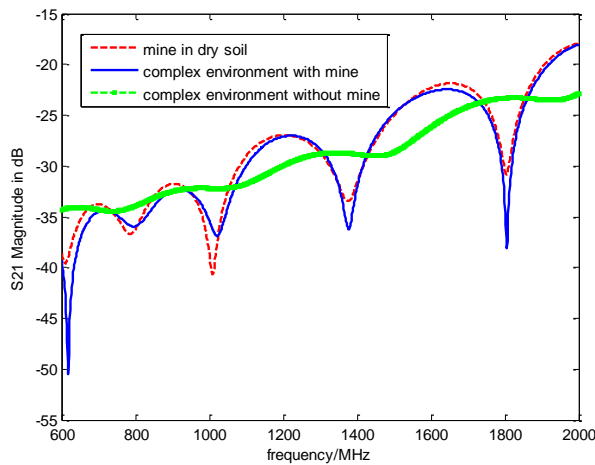
Fig. 10. Received signals for understanding the similarity between environments that landmine is present
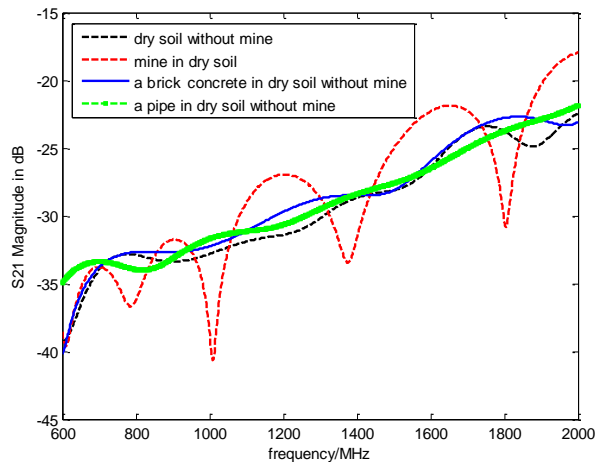
**Fig. 11.** Received signals for understanding the effect of soil in simulations

Now, we want to compare simulations together. A signal should be used as a reference signal for comparison. A 3-D plot of probability of detection (PD) according to the similarity and SNR is plotted in figure 12. A White

Gaussian Noise (WGN) has been added to the signal and then the similarity has been calculated according to SNR. In this paper, we define SNR according to the dB. The Number of Experiments (NE) to calculate PD is taken as:

$$NE = \frac{100}{error\%} \qquad (9)$$

Hence, NE for 0.01 % error is 10000 times [29].

Calculations for PD are done 100 times. When similarity in every calculation with constant SNR is more than threshold, the PD 1 percentage increases.
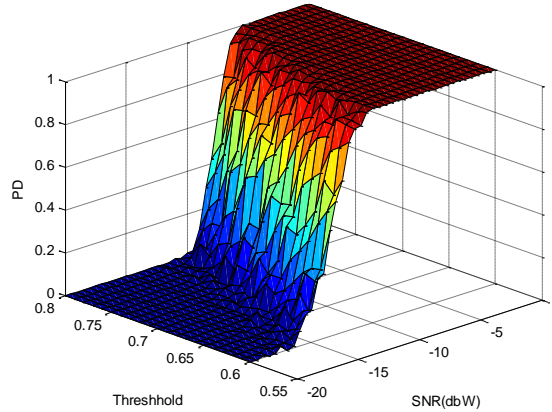
Fig. 12. PD when landmine is present

It is important that all landmines are found. Hence, probability of error (PE) according to the similarity and SNR is plotted in figure 13. Calculations for PE are done 100 times. When similarity in every calculation with constant SNR is more than threshold, PE 1 percentage increases. PE is done when the landmine is absent.
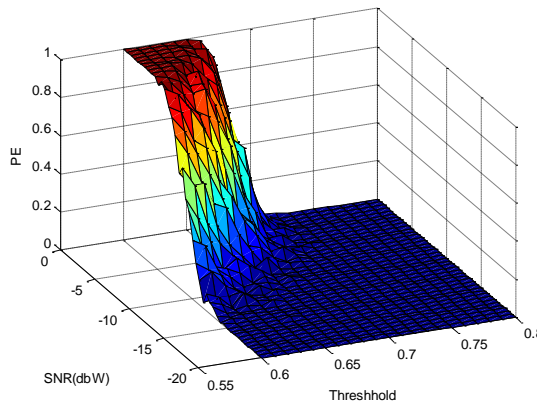
Fig. 13. PE when landmine is absent

The figure 13 demonstrates that if the threshold is more than 0.75 all of landmines are detectable.

5. CONCLUSION

In this paper, the detection in the presence of other objects is done. It is very important that your model can find the effect of landmine from other objects. The scattering parameter can be used for the detection of buried objects in the subsurface. The effect of noise is not considerable because landmine presence or absence effects are visible.

In this paper, we demonstrate that if the level of threshold decreases, SNR decreases and PE increases. Hence, the level of threshold must be optimum. This method is applicable where subsurface soil is dry. This method is not operating where the surface of soil is wet, for example in the tropical forest.

REFERENCES

[1] Park, S., Kim, K., & Ko, K. H. (2014). Multi-Feature Based Multiple Landmine Detection Using Ground Penetration Radar. Radioengineering, 23(2), 642–651.

[2] Caratelli, D., Yarovoy, A., & Ligthart, L. P. (2011). 'Full-Wave Modeling of Buried Pipe Detection with Low-Frequency Ground-Penetrating Radar. Στο Novel Applications of the UWB Technologies (σσ. 177–182). InTech.

[3] Bradford, J. H., Dickins, D. F., & Brandvik, P. J. (2010). Airborne GPR to Detect Oil under Snow (No. 24). SINTEF Report.

[4] Khuut, T. S. E. E. D. U. L. A. M. (2009). Application of Polarimetric GPR to detection of subsurface objects (Doctoral dissertation, Ph. D. dissertation, Dept. Elect. Eng. Tohoku Univ).

[5] Gurbuz, A. C., McClellan, J. H., & Scott, W. R. (2009). A compressive sensing data acquisition and imaging method for stepped frequency GPRs. IEEE transactions on signal processing: a publication of the IEEE Signal Processing Society, 57(7), 2640–2650. doi:10.1109/tsp.2009.2016270

[6] Yelf, R. J. (2007). Application of ground penetrating radar to civil and geotechnical engineering. Electromagnetic Phenomena, 7(1), 18.

[7] Stickley, G. F., Noon, D. A., Cherniakov, M., & Longstaff, I. D. (2000). Gated stepped-frequency ground penetrating radar. Journal of Applied Geophysics, 43(2–4), 259–269. doi:10.1016/s0926-9851(99)00063-4

[8] Porandla, R., Ravikanth, G., & Ramu, P. (2013). Power Optimization In Digital Circuits Using Scan-Based BIST. IJRCCT, 2(6), 339-346.

[9] Ismail, A., Elmogy, M., & ElBakry, H. (2014). Landmines Detection Using Autonomous Robots: A Survey. International Journal of Emerging Trends & Technology in Computer Science (IJETTCS), 3(4), 184-187.

[10] Haupt, R. W., & Rolt, K. D. (2005). Standoff acoustic laser technique to locate buried land mines. Lincoln Laboratory Journal, 15(1), 3-22.

[11] Takahashi, K., Igel, J., Preetz, H., & Sato, M. (2014). Influence of heterogeneous soils and clutter on the performance of ground-penetrating radar for landmine detection. IEEE transactions on geoscience and remote sensing: a publication of the IEEE Geoscience and Remote Sensing Society, 52(6), 3464–3472. doi:10.1109/tgrs.2013.2273082

[12] Kolba, M. P., & Jouny, I. I. (2004). Buried land mine detection using complex natural resonances on GPR data. IGARSS 2003. 2003 IEEE International Geoscience and Remote Sensing Symposium. Proceedings (IEEE Cat. No.03CH37477). Toulouse, France. doi:10.1109/igarss.2003.1293909

[13] Yang, C.-C., & Bose, N. K. (2005). Landmine detection and classification with complex-valued hybrid neural network using scattering parameters dataset. IEEE Transactions on Neural Networks, 16(3), 743–753. doi:10.1109/TNN.2005.844906

[14] Balan, A. N., & Azimi-Sadjadi, M. R. (1995). Detection and classification of buried dielectric anomalies by means of the bispectrum method and neural networks. IEEE transactions on instrumentation and measurement, 44(6), 998–1002. doi:10.1109/19.475145

[15] Azimi-Sadjadi, M. R., & Stricker, S. A. (1994). Detection and classification of buried dielectric anomalies using neural networks-further results. IEEE transactions on instrumentation and measurement, 43(1), 34–39. doi:10.1109/19.286352

[16] Plett, G. L., Doi, T., & Torrieri, D. (1997). Mine detection using scattering parameters. IEEE Transactions on Neural Networks, 8(6), 1456–1467. doi:10.1109/72.641468

[17] Ramm, A. G. (2005). Wave scattering by small bodies of arbitrary shapes (pp. 379-403). Springer US.

[18] Roberts, R. L., & Daniels, J. J. (1996). Analysis of GPR polarization phenomena. Journal of environmental & engineering geophysics, 1(2), 139–157. doi:10.4133/jeeg1.2.139

[19] Chew, K. M., Sudirman, R., Mahmood, N. H., Seman, N., & Yong, C. Y. (2013). Human brain microwave imaging signal processing: Frequency domain (S-parameters) to time domain conversion. Engineering, 05(05), 31–36. doi:10.4236/eng.2013.55b007

[20] Jamlos, M. A., Jamlos, M. F., & Ismail, A. H. (2015, May). High performance novel UWB array antenna for brain tumor detection via scattering parameters in microwave imaging simulation system. In Antennas and Propagation (EuCAP), 2015 9th European Conference on (pp. 1-5). IEEE.

[21] Jamlos, M.A. , Jamlos, M.F., Ismail, A.H.(2015). Lung Tumour Detection from a system of Scattering

Parameters. 9th European Conference on Antennas and Propagation (EuCAP), 1-5.

[22] Barton, D. K., & Leonov, S. A. (1998). Radar technology encyclopedia. Artech house.

[23] Pozar, D. M. (2009). Microwave engineering. John Wiley & Sons.

[24] Hejazi, M. A., Alehoseini, H. A., & Gharehpetian, G. B. (2010, Νοέμβριος). Detection of transformer winding axial displacement using scattering parameter and ANN. 2010 IEEE International Conference on Power and Energy. Kuala Lumpur, Malaysia. doi:10.1109/pecon.2010.5697606

[25] Carlson, A. B., Crilly, P. B., & Rutledge, J. C. Communication Systems, 2002.

[26] Gonzalez-Huici, M. A., Uschkerat, U., & Hoerdt, A. (2007). Numerical simulation of electromagnetic-wave propagation for land mine detection using GPR. 2007 IEEE International Geoscience and Remote Sensing Symposium. Barcelona, Spain. doi:10.1109/igarss.2007.4423974

[27] Gürbüz, A. C., McClellan, J. H., & Scott, W. R. (2006, May). Predicting GPR target locations using time delay differences. In Detection and Remediation Technologies for Mines and Minelike Targets XI (Vol. 6217, p. 621731). International Society for Optics and Photonics.

[28] Montoya, T. P., & Smith, G. S. (1999). Land mine detection using a ground-penetrating radar based on resistively loaded Vee dipoles. IEEE transactions on antennas and propagation, 47(12), 1795–1806. doi:10.1109/8.817655

[29] Papoulis, A., & Pillai, S. U. (2002). Probability, random variables, and stochastic processes. Tata McGraw-Hill Education.